Biomaterials Science

ROYAL SOCIETY OF CHEMISTRY

PAPER

View Article Online
View Journal | View Issue

Cite this: *Biomater. Sci.*, 2024, **12**, 4170

Unnatural lipids for simultaneous mRNA delivery and metabolic cell labeling†

Yusheng Liu,[a] Jiadiao Zhou,[a] Yueji Wang,[a] Dhyanesh Baskaran[a] and Hua Wang *[a,b,c,d,e,f,g]

Received 5th May 2024,
Accepted 25th June 2024

DOI: 10.1039/d4bm00625a

rsc.li/biomaterials-science

Lipids have demonstrated tremendous promise for mRNA delivery, as evidenced by the success of Covid-19 mRNA vaccines. However, existing lipids are mostly used as delivery vehicles and lack the ability to monitor and further modulate the target cells. Here, for the first time, we report a class of unnatural lipids (azido-DOTAP) that can efficiently deliver mRNAs into cells and meanwhile metabolically label cells with unique chemical tags (*e.g.*, azido groups). The azido tags expressed on the cell membrane enable the monitoring of transfected cells, and can mediate subsequent conjugation of cargos *via* efficient click chemistry for further modulation of transfected cells. We further demonstrate that the dual-functional unnatural lipid is applicable to different types of cells including dendritic cells, the prominent type of antigen presenting cells, potentially opening a new avenue to developing enhanced mRNA vaccines.

Introduction

Nucleic acid-based therapies have demonstrated tremendous promise for treating a variety of diseases, as evidenced by the great success of mRNA vaccines in the era of COVID-19.[1–3] The development of delivery vehicles that can stably and efficiently deliver nucleic acids into the target cells is essential for the success of nucleic acid-based therapies.[4] Among the various types of delivery vehicles developed to date, lipids have stood out for *in vitro* and *in vivo* delivery of nucleic acids.[5,6] For example, ionizable lipids and lipid nanoparticles were used as the delivery vehicle for SARS-Cov-2 mRNAs for the development of COVID-19 vaccines.[7–10] Lipofectamines have also become a gold standard for mRNA and plasmid delivery and *in vitro* transfection of numerous types of cells.[11,12] In these applications, lipids purely function as the delivery vehicle and require the incorporation of additional components to monitor the cellular uptake and transfection efficiency of cells.[7–12] Also, methods to further modulate the transfected cells, which could lead to enhanced efficacy for nucleic acid-based therapies, are lacking. Here, we aim to develop a class of unnatural lipids that can efficiently deliver nucleic acids into cells and further enable targeted modulation of transfected cells.

Lipids and sugars are two most abundant types of molecules on the cell membrane. By leveraging the cellular glycan synthesis machinery, the metabolic glycoengineering process of unnatural monosaccharides has provided a facile yet powerful tool to introduce unique chemical tags (*e.g.*, azido groups) onto the cell membrane.[13–17] The cell-surface azido groups then enable targeted conjugation of dibenzocyclooctyne (DBCO)-bearing cargos *via* efficient and bioorthogonal click chemistry. This two-step approach has been widely used for the imaging or targeted modulation of cancer cells, immune cells, and bacteria.[18–22] In contrast to the well-established metabolic glycan labeling method, effective methods to introduce unnatural lipids to the cell membrane *via* the metabolic lipid pathways are still lacking. Choline derivatives were shown to be metabolizable by cells and enable the chemical tagging of cells but are limited by the low labeling efficiency.[23–27] Primary alcohols bearing chemical tags can also convert phosphatidylcholine into phosphatidyl alcohols in the presence of phospholipase D, but only at concentrations >20 mM, which induce significant cytotoxic effects.[28–33]

Herein, we report a new class of unnatural lipids, 1,2-dioleoyl-3-azidoethyldimethylammoniumpropane (azido-DOTAP), that can complex with mRNAs, facilitate intracellular delivery

[a]*Department of Materials Science and Engineering, University of Illinois at Urbana-Champaign, Urbana, IL 61801, USA. E-mail: huawang3@illinois.edu*
[b]*Cancer Center at Illinois (CCIL), Urbana, IL 61801, USA*
[c]*Department of Bioengineering, University of Illinois at Urbana-Champaign, Urbana, IL 61801, USA*
[d]*Carle College of Medicine, University of Illinois at Urbana-Champaign, Urbana, IL 61801, USA*
[e]*Beckman Institute for Advanced Science and Technology, University of Illinois at Urbana-Champaign, Urbana, IL 61801, USA*
[f]*Materials Research Laboratory, University of Illinois at Urbana-Champaign, Urbana, IL 61801, USA*
[g]*Institute for Genomic Biology, University of Illinois at Urbana-Champaign, Urbana, IL 61801, USA*

†Electronic supplementary information (ESI) available. See DOI: https://doi.org/10.1039/d4bm00625a

of mRNAs, and meanwhile metabolically label cells with azido groups. This is built upon the phenomenon that cationic DOTAP can complex with negatively charged mRNA and, upon cellular internalization, can be hydrolyzed into 1,2-dihydroxyl-3-trimethylammoniumpropane in the presence of intracellular esterases.[34–36] The generated alcohol can then be metabolized *via* the lipid synthesis pathways and eventually become expressed on the cell membrane.[30–33] We hypothesize that the functionalization of DOTAP with azido groups, *via* the replacement of one methyl group with an azidoethyl group, could conserve the metabolic labeling ability and enable the metabolic tagging of cell membranes with azido groups (Fig. 1a).

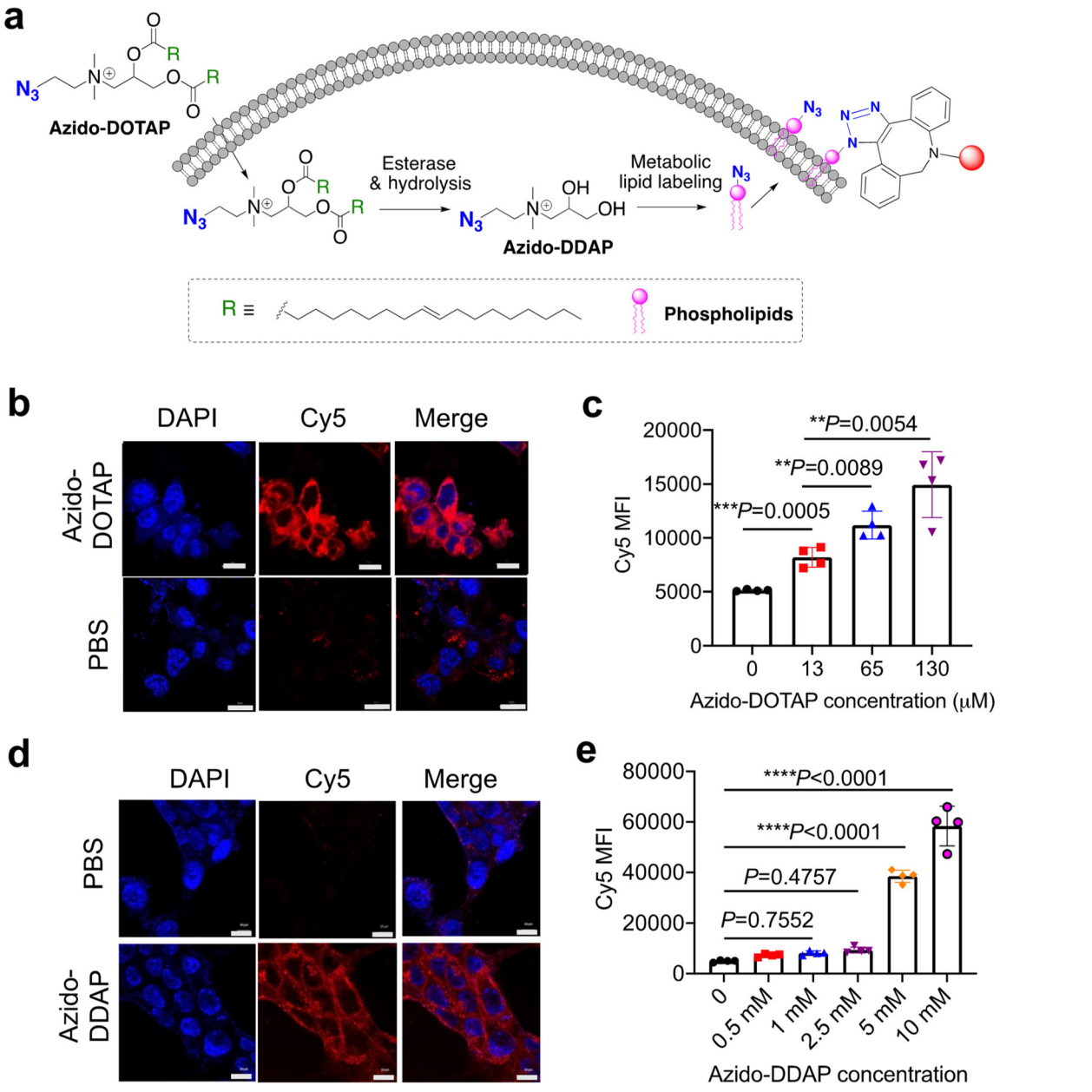

Fig. 1 Azido-DOTAP can metabolically label cells with azido groups. (a) Schematic illustration for the metabolic lipid labeling process of azido-DOTAP. Upon cellular internalization, azido-DOTAP can be hydrolyzed into azido-DDAP, which can undergo metabolic lipid engineering processes and become expressed on the cell membrane in the form of phospholipids. The cell-surface azido groups can then be detected with DBCO-Cy5 *via* efficient click chemistry. (b) CLSM images of 4T1 cells after 24 h incubation with azido-DOTAP (50 μM) or PBS and 20 min staining with DBCO-Cy5 (red). Nucleus was stained with DAPI (blue). Scale bar: 10 μm. (c) Mean Cy5 fluorescence intensity of 4T1 cells following the same treatment as in (b). (d) CLSM images of 4T1 cells after 24 h incubation with azido-DDAP (5 mM) or PBS and 20 min staining with DBCO-Cy5. Nucleus was stained with DAPI (blue). Scale bar: 10 μm. (e) Mean Cy5 fluorescence intensity of 4T1 cells following the same treatment as in (d). All the numerical data are presented as mean ± SD ($0.01 < {}^{*}P \leq 0.05$; $^{**}P \leq 0.01$; $^{***}P \leq 0.001$).

Results and discussion

Azido-DOTAP mediated metabolic labeling of cells

Prior to the synthesis of azido-DOTAP, we first synthesized 1,2-dihydroxyl-3-azidoethyldimethylammoniumpropane (azido-DDAP) *via* the complexation of 3-chloro-1,2-propanediol and 2-azido-*N*,*N*′-dimethylethanamine (Fig. 1a and Fig. S1†). Azido-DDAP was further reacted with oleoyl chloride to yield azido-DOTAP (Fig. 1a and Fig. S1†). The chemical structure of azido-DDAP and azido-DOTAP was well characterized by ^{1}H NMR and ^{13}C NMR spectrometry (Fig. S2 and 3†). We also performed FTIR spectrometry of azido-DOTAP and DOTAP. The presence of the 2106 cm^{-1} peak confirmed the presence of azido groups in azido-DOTAP (Fig. S4†). To study whether azido-DOTAP can metabolically label cells with azido groups (Fig. 1a), 4T1 breast cancer cells were incubated with azido-DOTAP for 24 h, followed by 20 min incubation with DBCO-Cy5 to detect the cell-surface azido groups *via* efficient click chemistry. Compared to control cells without azido-DOTAP treatment, cells treated with azido-DOTAP exhibited a much brighter Cy5 fluorescence signal on the cell membrane (Fig. 1b), indicating the successful metabolic labeling of 4T1 cells with azido groups. Flow cytometry analysis confirmed the concentration-dependent azido tagging of 4T1 cells by azido-DOTAP (Fig. 1c). We also tested the metabolic labeling capability of azido-DDAP, a potential hydrolysis product of azido-DOTAP. Compared to 4T1 cells pretreated with PBS, cells pretreated with azido-DDAP showed a higher Cy5 fluorescence intensity (Fig. 1d and e), indicating the successful labeling of cells with azido groups. However, compared to azido-DOTAP, a much higher concentration of azido-DDAP was needed to achieve a notable labeling effect (Fig. 1d and e), presumably due to the lower cell uptake of azido-DDAP than azido-DOTAP. This is consistent with previous reports indicating that hydroxyl-exposed monosaccharides exhibit a lower cellular uptake than acetylated monosaccharides.[37,38] By incubating 4T1 cells with 25 or 50 μM azido-DOTAP, azido-DDAP, and azido-choline for 24 h and staining cells with DBCO-Cy5, the azido-DOTAP group showed a significantly higher Cy5 fluorescence intensity than azido-DDAP and azido-choline groups, demonstrating the superior metabolic labeling effect of azido-DOTAP over azido-DDAP and azido-choline (Fig. S5†). The cyto-

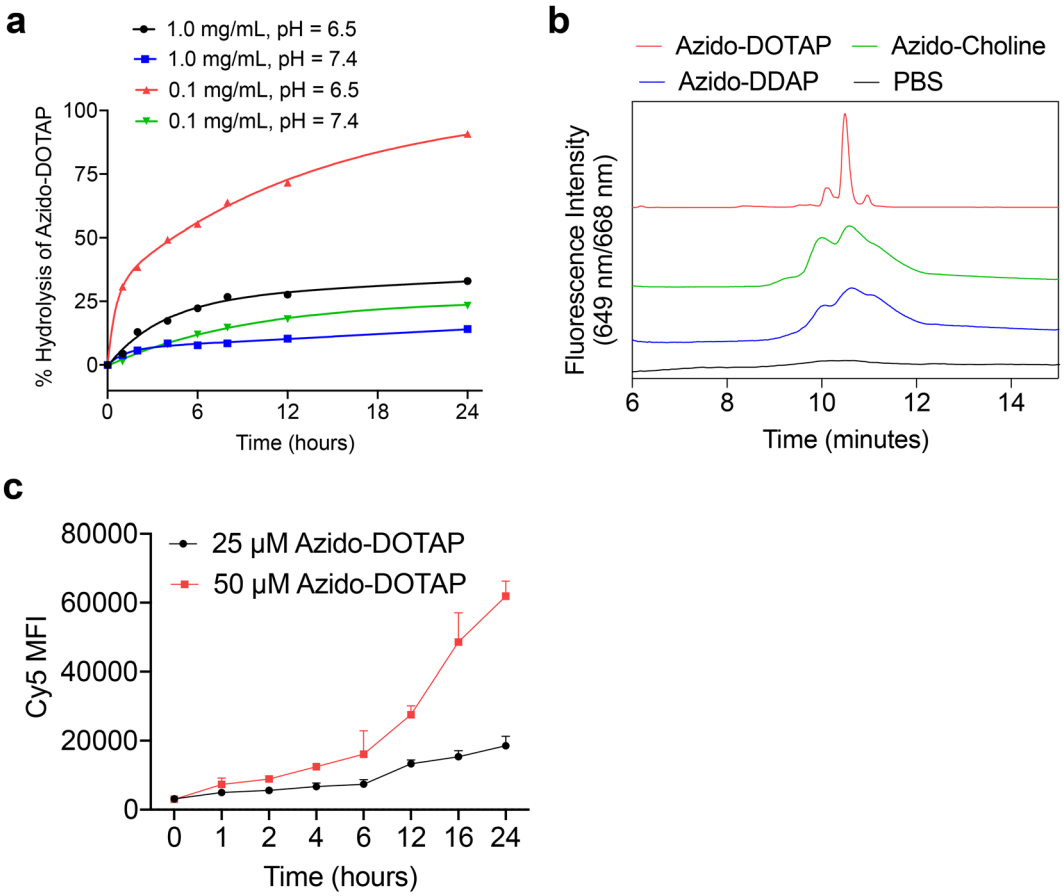

Fig. 2 Azido-DOTAP can be hydrolyzed into azido-DDAP and become metabolically incorporated into membrane lipids. (a) Hydrolysis kinetics of azido-DOTAP at pH 6.5 and 7.4, respectively. The concentration of azido-DOTAP was set at 1.0 or 0.1 mg mL^{-1}. (b) HPLC profiles (fluorescence mode) of membrane lipids that were extracted from 4T1 cells pretreated with azido-DOTAP (25 μM), azido-choline (2 mM), azido-DDAP (2 mM), and PBS, respectively, for 24 h. The extracted lipids were incubated with DBCO-Cy5 prior to HPLC runs. (c) Mean Cy5 fluorescence intensity of 4T1 cells after treating with 25 or 50 μM azido-DOTAP for different times and staining with DBCO-Cy5.

toxicity of azido-DOTAP, DOTAP, azido-DDAP, and azido-choline against 4T1 cells was analyzed *via* the MTT assay, which showed IC_{50} values of 86.2 μM, 42.1 μM, 14.7 mM, and 5.1 mM, respectively (Fig. S6†). We also confirmed the pH-dependent hydrolysis of azido-DOTAP into azido-DDAP. At pH 7.4 and 0.1 mg mL^{-1}, ~10% of azido-DOTAP was hydrolyzed into azido-DDAP over 24 h (Fig. 2a). At pH 6.5 and 0.1 mg mL^{-1}, azido-DOTAP exhibited a much higher hydrolysis rate, with >90% degradation over 24 h (Fig. 2a). Azido-DOTAP showed a slower hydrolysis rate at a higher concentration (1 mg mL^{-1}), but the hydrolysis was still pH-dependent (Fig. 2a). Considering the acidity of endosomes, we expect the rapid degradation of azido-DOTAP into azido-DDAP upon cellular internalization.

To further validate the metabolic lipid labeling, we extracted the lipid molecules from cells pretreated with azido-DOTAP, azido-DDAP, azido-choline, or PBS for 24 h, then incubated them with DBCO-Cy5 for 20 min, and ran the samples on HPLC. As the negative control, lipids extracted from PBS-treated cells showed minimal Cy5 signal (Fig. 2b). In comparison, cells pretreated with azido-choline, azido-DOTAP, or azido-DDAP and then incubated with DBCO-Cy5 contained

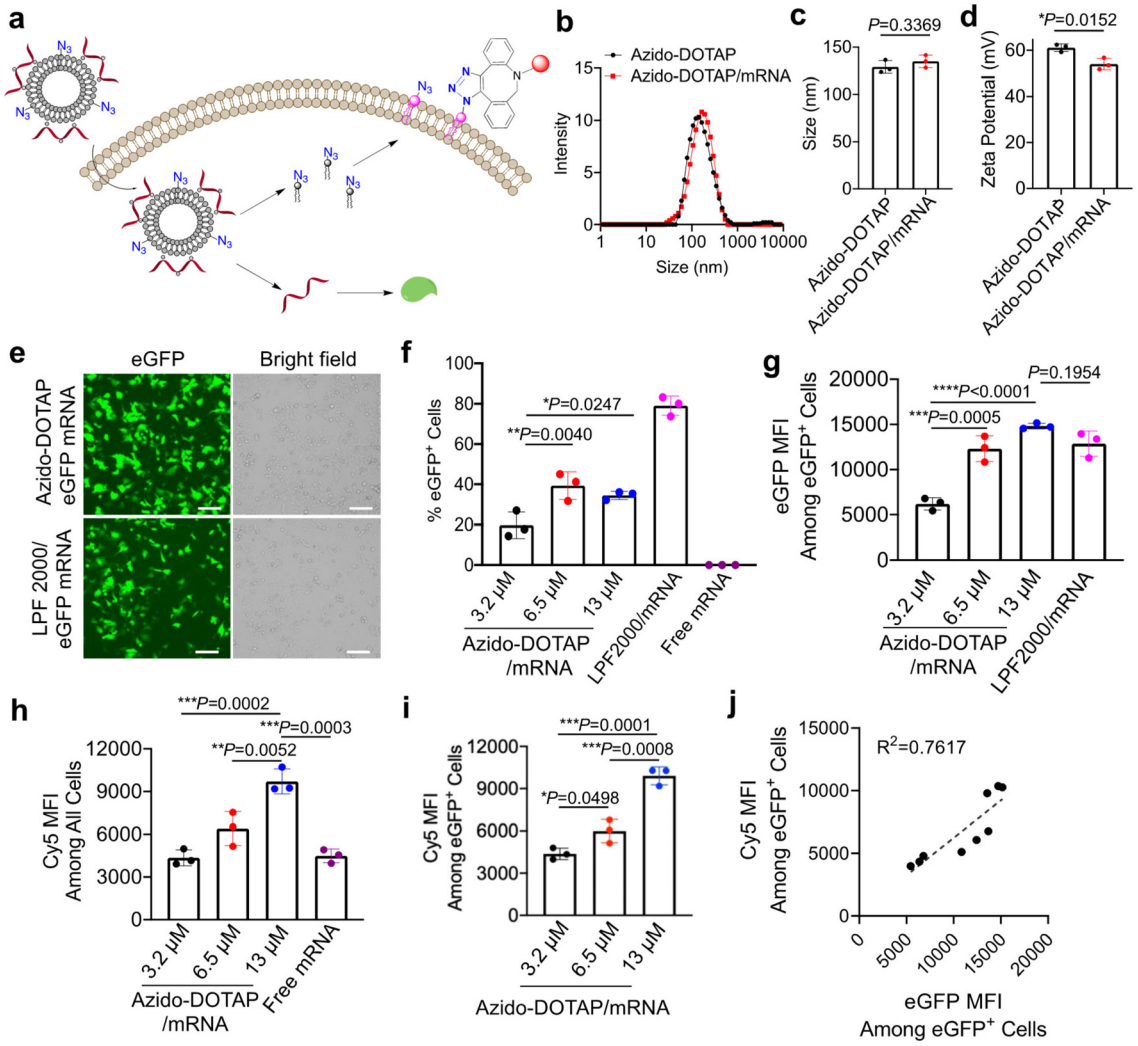

Fig. 3 Azido-DOTAP/mRNA complexes can simultaneously transfect cells and metabolically label cells with azido groups. (a) Schematic illustration of azido-DOTAP/eGFP mRNA mediated cell transfection and labeling. (b) Dynamic light scattering (DLS) profile, (c) size, and (d) zeta potential of azido-DOTAP nanoparticles and azido-DOTAP/mRNA complexes. (e) CLSM images of HEK293T cells after incubation with azido-DOTAP/eGFP mRNA complexes or lipofectamine/eGFP mRNA complexes for 48 h. The mass ratio of lipid to mRNA was fixed at 5 : 1. Scale bar: 100 μm. (f) % $eGFP^+$ HEK293T cells after treatment with different groups for 48 h. The concentration of mRNA was fixed at 1 μg mL^{-1}. The concentration of azido-DOTAP was 3.2 μM (2.5 μg mL^{-1}), 6.5 μM, or 13 μM. 5 μg mL^{-1} LPF2000 was used. (g) Mean eGFP fluorescence intensity among $eGFP^+$ HEK293T cells after 48 h treatment with different groups. Also shown is the mean Cy5 fluorescence intensity (h) among all HEK293T cells or (i) among $eGFP^+$ HEK293T cells after 48 h treatment with different groups and staining with DBCO-Cy5. (j) Correlation of Cy5 MFI and eGFP MFI among $eGFP^+$ cells. All the numerical data are presented as mean ± SD ($0.01 < *P \leq 0.05$; $**P \leq 0.01$; $***P \leq 0.001$).

Cy5-tagged lipids, substantiating the successful azido labeling of cells by azido-choline, azido-DOTAP, or azido-DDAP (Fig. 2b). To better understand the metabolic labeling kinetics of azido-DOTAP, we incubated 4T1 cells with azido-DOTAP for different times and then detected cell-surface azido groups with DBCO-Cy5. Cell-surface azido groups became detectable after 1–2 h, and the density gradually increased over the course of 24 h (Fig. 2c). By increasing the concentration of azido-DOTAP, the metabolic labeling kinetics follows a similar trend, albeit at a higher labeling efficiency (Fig. 2c). This accumulative labeling kinetics matches with the kinetics of intracellular metabolic lipid engineering processes instead of direct lipid insertion into cell membranes, which often happens within minutes after adding the lipids. These experiments demonstrated that azido-DOTAP can be hydrolyzed into azido-DDAP and, *via* incubation with 4T1 cells, can be metabolically incorporated into membrane lipids.

Azido-DOTAP mediated simultaneous mRNA delivery and cell tagging

We next studied the capability of azido-DOTAP to condense and stably deliver mRNAs into cells. In accordance with the commonly used protocol for preparing lipofectamine/mRNA complexes (Fig. S7a–c†), we formulated the nanoparticulate azido-DOTAP *via* the extrusion method and then condensed it with eGFP-encoding mRNA to form the complex (Fig. 3a). Dynamic light scattering showed a diameter of ~130 nm (Fig. 3b and c) and a surface charge of ~52 mV (Fig. 3d) for the complexes formed at an azido-DOTAP : mRNA mass ratio of 5 : 1. The increase in the size and the decrease in the surface charge of azido-DOTAP/mRNA complexes, in comparison with azido-DOTAP nanoparticles, indicated the successful incorporation of mRNA (Fig. 3b–d). The agarose gel electrophoresis results also confirmed the successful incorporation of mRNAs

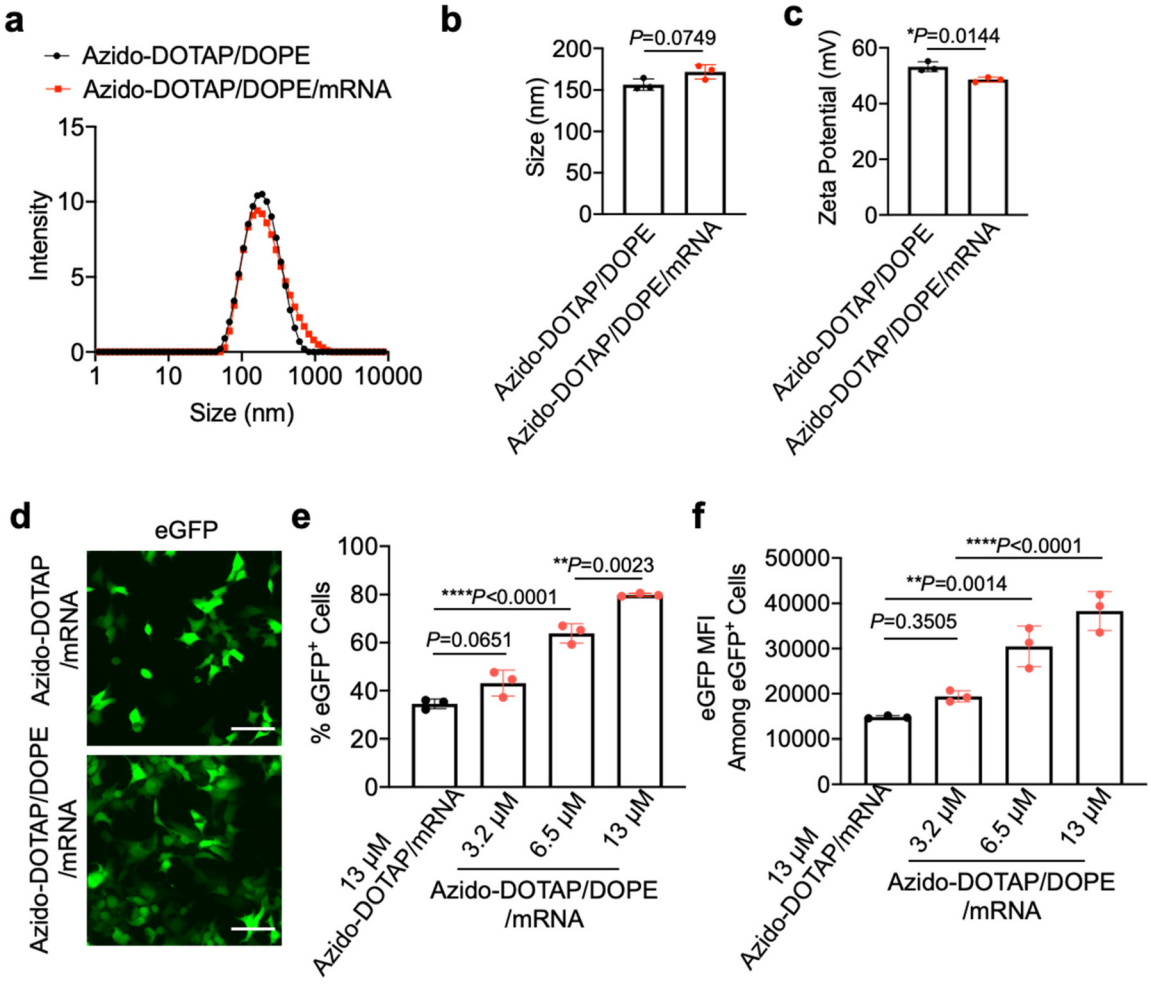

Fig. 4 Incorporation of DOPE increases the transfection efficiency of azido-DOTAP/mRNA complexes. (a) DLS profile, (b) size, and (c) zeta potential of azido-DOTAP/DOPE nanoparticles and azido-DOTAP/DOPE/mRNA complexes. The molar ratio of azido-DOTAP to DOPE was 6 : 4. The mass ratio of lipid to mRNA was set at 5 : 1. (d) CLSM images of HEK293T cells after 48 h incubation with azido-DOTAP/mRNA complexes or azido-DOTAP/DOPE/mRNA complexes. Scale bar: 50 μm. (e) % eGFP$^+$ HEK293T cells after 48 h treatment with different groups. The concentration of mRNA was fixed at 1 μg mL^{-1}. The molar ratio of azido-DOTAP to DOPE was 6 : 4. (f) Mean eGFP fluorescence intensity of eGFP$^+$ HEK293T cells after 48 h treatment with different groups. All the numerical data are presented as mean ± SD ($0.01 < *P \leq 0.05$; $**P \leq 0.01$; $***P \leq 0.001$).

into the complexes (Fig. S8†). The formed azido-DOTAP/mRNA complexes were stable under physiological conditions for over 48 h, as evidenced by the negligible changes in size and zeta potential (Fig. S9a–c†). After incubating HEK293T cells with the complexes for 48 h, strong eGFP fluorescence intensity was observed in cells treated with azido-DOTAP/mRNA complexes (Fig. 3e), indicating the successful expression of eGFP mRNA. Flow cytometry analyses confirmed the concentration-dependent transfection efficiency of azido-DOTAP/eGFP mRNA complexes (Fig. 3f and g). We also incubated azido-DOTAP/mRNA

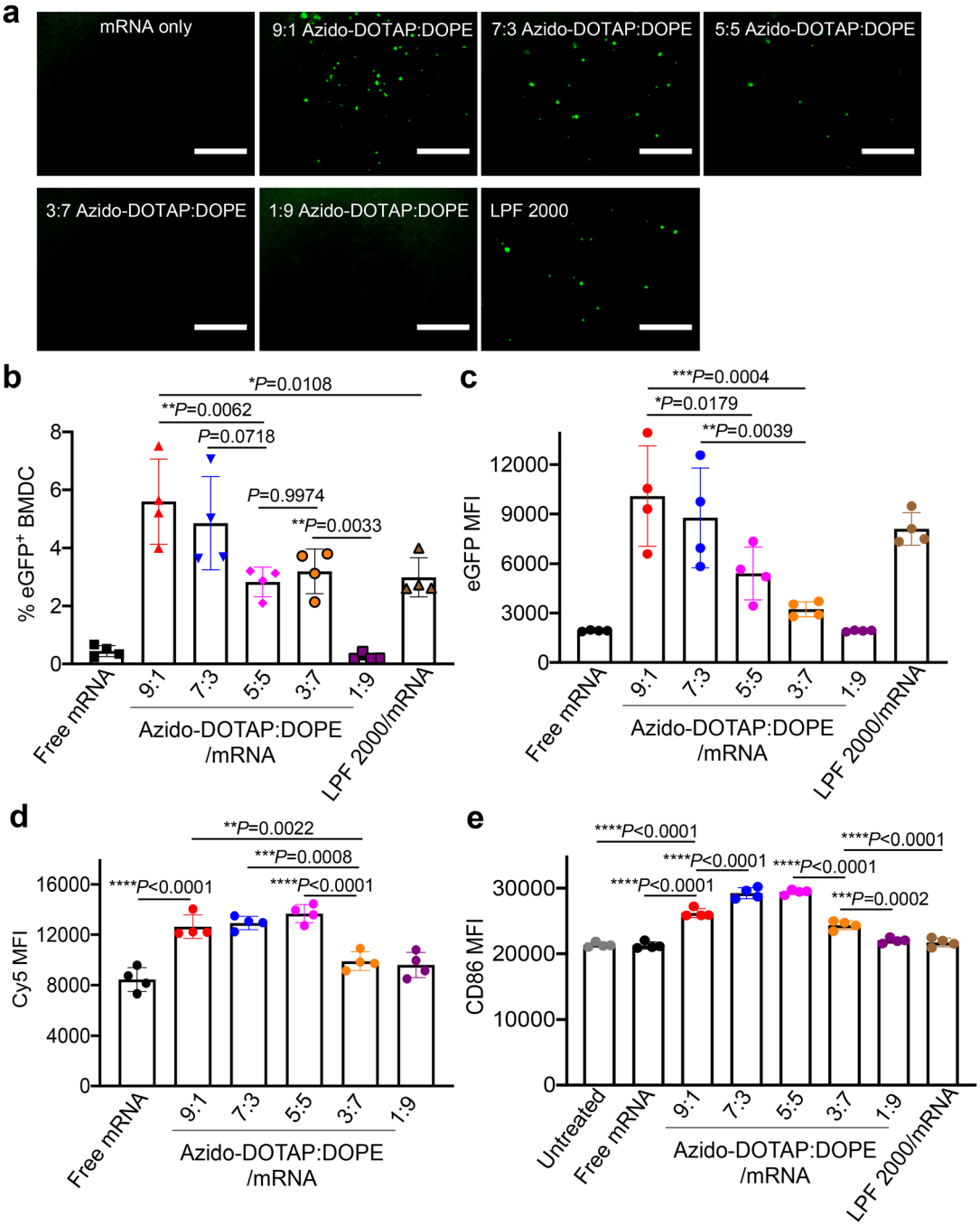

Fig. 5 Azido-DOTAP/DOPE/mRNA complexes enable simultaneous transfection, metabolic tagging, and activation of dendritic cells. (a) Fluorescence images of BMDCs after 48 h treatment with azido-DOTAP/DOPE/mRNA complexes with varied azido-DOTAP : DOPE molar ratios. Scale bar: 300 μm. The mass ratio of lipid to mRNA was fixed at 10 : 1 for all groups. (b) % $eGFP^+$ BMDCs after 48 h treatment with different groups. (c) Mean eGFP fluorescence intensity of BMDCs after 48 h treatment with different groups. (d) Mean Cy5 fluorescence intensity of BMDCs after 48 h treatment with different groups and staining with DBCO-Cy5. (e) Mean CD86 fluorescence intensity of BMDCs after 48 h treatment with different groups and staining with PE/Cy7-conjugated anti-CD86. All the numerical data are presented as mean ± SD ($0.01 < *P \leq 0.05$; $**P \leq 0.01$; $***P \leq 0.001$).

complexe-pretreated cells with DBCO-Cy5 for 20 min, in order to detect the potentially expressed azido groups on the cell membrane. As expected, cells treated with azido-DOTAP/mRNA complexes showed a higher Cy5 fluorescence intensity than control cells (Fig. 3h and i), demonstrating the successful metabolic labeling of cells with azido groups. Further analysis confirmed a good correlation between the eGFP signal and the Cy5 signal (R^2 = 0.7617, Fig. 3j). These experiments demonstrated the ability of azido-DOTAP to function as an effective delivery vehicle for mRNAs and meanwhile metabolically label cells with azido groups.

Incorporation of DOPE enhances the transfection efficiency

We further studied whether the incorporation of additional helper lipids such as dioleoylphosphatidylethanolamine (DOPE) can tune the transfection efficiency while maintaining the metabolic labeling ability. We mixed DOPE and azido-DOTAP at a molar ratio of 6 : 4 and complexed them with eGFP mRNA. The increase of size and the decrease of surface charge (Fig. 4a–c), as well as the agarose gel electrophoresis result (Fig. S8†), confirmed the successful incorporation of mRNA into the complexes. HEK293T cells were then incubated with the complexes with lipid : mRNA mass ratios of 2.5 : 1 (3.2 μM lipid), 5 : 1 (6.5 μM lipid), and 10 : 1 (13 μM lipid), respectively, for 48 h, followed by the detection of eGFP expression *via* fluorescence microscopy and flow cytometry. Fluorescence images showed the successful expression of eGFP in cells treated with azido-DOTAP/mRNA or azido-DOTAP/DOPE/mRNA (Fig. 4d). Compared to azido-DOTAP, the mixture of azido-DOTAP and DOPE resulted in the improved transfection efficiency of eGFP mRNA in HEK293T cells (Fig. 4e and f). These experiments demonstrated the feasibility of enhancing the transfection efficiency of azido-DOTAP/mRNA complexes.

Simultaneous transfection and metabolic labeling of dendritic cells

To extend the applicability of azido-DOTAP to different types of cells, we next studied whether azido-DOTAP/DOPE/mRNA complexes can simultaneously transfect and metabolically label bone marrow-derived dendritic cells (BMDCs), the prominent type of antigen presenting cells in the body. We mixed different molar ratios of azido-DOTAP and DOPE (9 : 1, 7 : 3, 5 : 5, 3 : 7, and 1 : 9, respectively) and then incubated them with eGFP mRNA with a lipid : mRNA mass ratio of 10 : 1 to form the complexes. The mRNA complexes were incubated with murine BMDCs for 48 h, followed by fluorescence imaging and flow cytometry. Compared to cells treated with free mRNA, BMDCs treated with the complexes with a azido-DOTAP/DOPE molar ratio of 9 : 1, 7 : 3, 5 : 5, or 3 : 7 showed a much higher eGFP fluorescence intensity (Fig. 5a). DOTAP/DOPE/mRNA complexes with a 9 : 1 DOTAP/DOPE molar ratio also resulted in a higher transfection efficiency than the lipofectamine complex (Fig. 5a). Flow cytometry analyses also confirmed the much higher transfection efficiency of DOTAP/DOPE/mRNA complexes than that of free mRNAs and the correlation of transfection efficiency to DOTAP/DOPE molar ratios (Fig. 5b and c). We also analyzed the cell-surface azido groups as a result of the metabolic lipid labeling of azido-DOTAP. Azido-DOTAP/DOPE/mRNA complexes with a DOTAP/DOPE molar ratio of 9 : 1, 7 : 3, or 5 : 5 managed to label BMDCs with a detectable level of azido groups (Fig. 5d), which is consistent with the concentration dependent labeling effect of azido-DOTAP. We also compared azido-DOTAP and DOTAP for intracellular transfection of eGFP mRNA in BMDCs. At a concentration of 3.2 or 6.5 μM, azido-DOTAP/mRNA and DOTAP/mRNA showed a similar eGFP transfection efficiency in BMDCs (Fig. S10a†). At a concentration of 13 or 26 μM, azido-DOTAP/mRNA exhibited a slightly higher eGFP transfection efficiency than DOTAP/mRNA (Fig. S10a†), which is likely attributed to the difference in the chemical structure of azido-DOTAP and DOTAP. The same trend also applies to azido-DOTAP/DOPE/mRNA *versus* DOTAP/DOPE/mRNA (Fig. S10b†). Interestingly, azido-DOTAP/DOPE/mRNA complexes also upregulated the surface expression of CD86, a well-known activation marker of DCs, by BMDCs (Fig. 5e), likely due to the interactions between lipids and the DC membrane. The CD86 level was indeed well correlated to the azido labeling efficiency and transfection efficiency of DOTAP/DOPE/mRNA complexes (Fig. 5e). We also synthesized SIINFEKL antigen-encoding mRNA and complexed it with azido-DOTAP, azido-DOTAP/DOPE, or LPF2000. These complexes successfully transfected BMDCs with the SIINFEKL antigen and resulted in the presentation of MHCI-SIINFEKL on BMDCs (Fig. S11a and b†). The SIINFEKL antigen presentation efficiency increased with the concentration of azido-DOTAP (Fig. S11a and b†). To further confirm the role of azido-DOTAP in CD86 upregulation of DCs, BMDCs were treated with DOTAP/mRNA (encode for SIINFEKL), azido-DOTAP/mRNA, azido-DOTAP/DOPE/mRNA, DOTAP/mRNA, and DOPE mRNA, respectively. At 13 μM azido-DOTAP or DOTAP, compared to DOPE/mRNA, azido-DOTAP/mRNA, DOTAP/mRNA, azido-DOTAP/DOPE/mRNA, and DOTAP/DOPE/mRNA all resulted in a higher expression level of CD86 on DCs (Fig. S12†), substantiating the DC-activating effect of azido-DOTAP and DOTAP. Interestingly, compared to DOTAP/mRNA, azido-DOTAP/mRNA also induced higher CD86 expression on DCs (Fig. S12†).

Conclusion

In summary, we report a class of unnatural lipids that can condense and stably deliver mRNA into cells and meanwhile metabolically label cells with clickable chemical tags. We demonstrated the ability of azido-DOTAP to induce the efficient transfection of mRNAs in various types of cells including 4T1 breast cancer cells, HEK293T kidney cells, and BMDCs, while installing azido groups on the cell membrane. We further demonstrated that additional lipids can be incorporated to improve the overall transfection efficiency while maintaining the metabolic labeling capability. The cell-surface azido groups enable targeted conjugation of molecules or materials *via* efficient click chemistry to further modulate the function of transfected

cells. For the first time, we show that cationic lipids not only can deliver nucleic acids but also function as a labeling reagent for the monitoring and manipulation of target cells.

Methods

Materials and instrumentation

All chemicals used for the synthesis of lipids, including 3-chloro-1,2-propanediol, 2-azido-*N,N*-dimethylethanamine, and oleoyl chloride, were purchased from Sigma-Aldrich (St Louis, MO, USA) unless otherwise noted. Fetal Bovine Serum (FBS) was purchased from Thermo Fisher (Waltham, MA, USA). GM-CSF was purchased from PeproTech (Cranbury, NJ, USA). Primary antibodies used in this study, including FITC-conjugated anti-CD11c (Invitrogen) and PE/Cy7-conjugated anti-CD86 (Invitrogen), were purchased from Thermo Fisher Scientific (Waltham, MA, USA). Fixable viability dye efluor780 was obtained from Thermo Fisher Scientific (Waltham, MA, USA). All antibodies were diluted according to the manufacturer's recommendations. Small molecule compounds were run on the Agilent 1290/6140 ultra-high performance liquid chromatography/mass spectrometer or the Shimadzu high performance liquid chromatography system. Proton and carbon nuclear magnetic resonance spectra were collected on the Varian U500 or VXR500 (500 MHz) spectrometer. Fluorescence images were taken using an EVOS microscope (Thermo Fisher, Waltham, MA, USA). The confocal image was obtained using LSM 900 (ZEISS, USA). FACS data were collected using Attune NxT flow cytometers and analyzed with Flowjo™ 10. Statistical testing was performed using GraphPad Prism v8.

Cell lines

The 4T1 and HEK293T cell lines were purchased from American Type Culture Collection (Manassas, VA, USA). Cells were cultured in DMEM containing 10% FBS and 100 units per mL penicillin/streptomycin at 37 °C in 5% CO_2 humidified air.

Synthesis of azido-DDAP

3-Chloro-1,2-propanediol (1.1 g, 0.01 mol, 1.0 eq.) was dissolved in 5 mL of DI water, followed by the addition of 2-azido-*N,N*-dimethylethanamine (1.25 g, 0.011 mol, 1.1 eq.). The reaction mixture was heated to 60 °C and stirred for 12 hours until the complete consumption of 3-chloro-1,2-propanediol as monitored by HPLC. The solvent and residual 2-azido-*N,N*-dimethylethanamine were removed by rotary evaporation and lyophilization. ^{1}H NMR (500 MHz, D_2O): δ 4.32 (dtd, J = 8.4, 5.4, 2.9 Hz, 1H), 3.99 (t, J = 5.6 Hz, 2H), 3.73 (tt, J = 5.8, 3.5 Hz, 2H), 3.62 (d, J = 5.4 Hz, 2H), 3.58–3.50 (m, 2H), 3.28 (d, J = 6.7 Hz, 6H). ^{13}C NMR (500 MHz, D_2O) δ 66.95, 66.34, 63.85, 63.53, 52.61, 44.80.

Synthesis of azido-DOTAP

Azido-DDAP (0.5 g, 2.2 mmol) was dissolved in anhydrous dimethylformaldehyde (DMF), followed by the dropwise addition of oleoyl chloride (1.45 g, 4.8 mmol, 1.1 eq.) and triethylamine (0.5 g, 4.8 mmol, 1.1 eq.) in dimethylformaldehyde. The reaction mixture was stirred at 40 °C overnight. Then, DMF was removed using a rotavapor, and the residue was dissolved in dichloromethane. The crude product was purified by silica column chromatography with hexane and ethyl acetate as the eluent. Azido-DOTAP was obtained as a slight yellow solid. ^{1}H NMR (500 MHz, $CDCl_3$): δ 5.66–5.59 (m, 1H), 5.41–5.27 (m, 4H), 4.59–4.46 (m, 2H), 4.17–4.02 (m, 5H), 3.88 (dd, J = 14.4, 8.7 Hz, 1H), 3.51 (d, J = 6.8 Hz, 6H), 2.37–2.28 (m, 4H), 2.00 (t, J = 6.1 Hz, 8H), 1.63–1.54 (m, 4H), 1.28 (dp, J = 22.1, 7.0 Hz, 40H), 0.91–0.84 (m, 6H). ^{13}C NMR (126 MHz, $CDCl_3$): δ 173.34, 172.94, 130.14, 130.11, 129.76, 129.72, 65.92, 63.76, 63.45, 45.41, 34.31, 34.01, 32.00, 29.86, 29.63, 29.42, 29.36, 29.33, 29.28, 29.22, 29.18, 27.32, 27.29, 24.85, 24.76, 22.78, 14.22.

Confocal imaging of azido-DOTAP labeled cells

10^5 4T1 or HEK293T cells (1 mL of medium) were seeded onto the coverslips placed in a 6-well plate and allowed to attach to the coverslips for 12 h. Azido-DOTAP was then added to the cells. After 24 hours, the medium was removed, and cells were washed three times with PBS, and then DBCO-Cy5 (5 μg mL^{-1}) in FACS buffer (2% FBS in PBS) was added and incubated with cells for 20 min. Cells were then washed, stained with DAPI, and fixed with 4% PFA. Then the coverslips bearing the cells were transferred to microscope slides with the addition of ProLong™ Gold and stored at 4 °C prior to imaging.

Flow cytometry analysis of azido-DOTAP labeled cells

4T1 cells were treated with azido-DOTAP, azido-DDAP, azido-choline, or PBS for 24 h. Cells were then detached by treatment with 0.25% trypsin and washed three times with cold PBS. Cells were resuspended in FACS buffer with 5 μg mL^{-1} DBCO-Cy5 and eFluor™ 780 Fixable Viability Dye for 20 min. After washing, cells were suspended in FACS buffer containing 0.4% PFA and stored at 4 °C prior to flow cytometry analysis.

MTT assay

4T1 cells were seeded into 96-well plates and allowed to attach overnight. After washing, azido-DOTAP, DOTAP, azido-DDAP, and azido-choline at different final concentrations were then added. After 72 h, cells were washed three times with PBS, and MTT solution was added to each well and incubated with cells for 4 h. Dimethyl sulfoxide was then added and the plates were shaken for 10 minutes, prior to the absorbance measurement using a plate reader.

Extraction of lipids from cells for HPLC analysis

10^6 4T1 cells were seeded into a Petri dish in 10 mL medium and allowed to attach and proliferate. At ~60% confluency, 25 μM azido-DOTAP was added. After 24 hours, cells were detached by treatment with 0.25% trypsin and washed with PBS to remove non-specifically bound lipids. Cells were resuspended in cold FACS buffer containing 5 μg mL^{-1} DBCO-Cy5 for an hour at 4 °C. After washing three times with cold FACS buffer and twice with cold PBS, cells were re-suspended in

100 μL of water in a tube, followed by the addition of 150 μL of methanol/chloroform (2 : 1 volume ratio). The mixture was sonicated on ice for 10 minutes and then centrifuged at 12 000*g* for 5 minutes at 4 °C. The lower organic phase was carefully collected for HPLC analysis.

Release kinetic study of azido-DOTAP

Azido-DOTAP was dissolved in 200 μL of citric acid buffer (pH = 6.5) or PBS (pH = 7.4) with a final concentration of 0.1 mg mL^{-1} and 1.0 mg mL^{-1}, respectively. Then, the vials were placed at 37 °C, and 5 μL aliquots were taken at selected time points for HPLC analysis.

In vitro labeling kinetic study of azido-DOTAP

10^4 4T1 cells were seeded into 96-well plates in 0.1 mL medium and allowed to attach overnight. Azido-DOTAP (25 or 50 μM) was added at different times prior to flow cytometry analysis. Cells were washed three times with PBS, followed by the addition of DBCO-Cy5 (5 μg mL^{-1}) in FACS buffer. After washing three times with PBS, cells were lifted with trypsin, further washed twice with PBS, and resuspended in FACS buffer containing 0.4% PFA for flow cytometry analysis.

Azido-DOTAP mediated *in vitro* mRNA transfection

Azido-DOTAP (1 mg) was dissolved in chloroform. Chloroform was then removed using a rotavapor to form a thin lipid film, followed by lyophilization for 2 hours to completely remove chloroform. Biological grade water (1 mL) was then added, followed by sonication on ice. The mixture was extruded using the Avanti Extruder (100 nm membrane) to yield the lipid nanoparticles. Azido-DOTAP/DOPE nanoparticulates were prepared following a similar protocol, except for the replacement of azido-DOTAP with the mixture of azido-DOTAP and DOPE in the beginning. Azido-DOTAP or azido-DOTAP/DOPE was then complexed with eGFP-encoding mRNA at a lipid : mass ratio of 2.5 : 1, 5 : 1, or 10 : 1. For cell transfection, HEK293T cells were seeded in 96-well plates with 10 000 cells each well. Azido-DOTAP/mRNA complexes, azido-DOTAP/DOPE/mRNA complexes, or lipofectamine 2000/mRNA complexes were added to the wells. 100 ng of eGFP mRNA was added per well. Note that the lipofectamine/mRNA was purchased from a commercial vendor. According to the concentration information and the protocol provided by the vendor, we used a lipofectamine 2000 : mRNA mass ratio of 5 : 1 for the transfection studies. After 48 hours, cells were imaged under a fluorescence microscope. For flow cytometry analysis, cells were also stained with DBCO-Cy5 in FACS buffer, detached with trypsin, washed, and resuspended in FACS buffer.

BMDC transfection and labeling

BMDCs were differentiated from bone marrow cells following a previously reported protocol. Briefly, bone marrow cell suspensions were cultured in the presence of 20 ng mL^{-1} GM-CSF for 7 days and then cultured in the presence of 10 ng mL^{-1} GM-CSF. For the transfection experiments, BMDCs were seeded into 96-well plates at a density of 10k per well (100 μL medium). The complexes of eGFP mRNA and lipids (azido-DOTAP, the mixture of azido-DOTAP and DOPE, or lipofectamine 2000) were added to the cells (100 ng eGFP mRNA per well). The mass ratio of lipid : mRNA was fixed at 10 : 1 for the DC transfection studies. After 48 hours, cells were imaged under a fluorescence microscope. For flow cytometry analysis, cells were also stained with DBCO-Cy5 in FACS buffer first, washed, and resuspended in FACS buffer. Then FITC-conjugated anti-CD11c, PE/Cy7-conjugated anti-CD86 and fixable viability dye efluor780 were added to cells. After staining for 30 minutes, cells were washed and resuspended in FACS buffer containing 0.4% PFA for flow cytometry analysis.

Comparison of azido-DOTAP and DOTAP for mRNA transfection

Day-7 BMDCs were seeded into 96-well plates at a density of 10k per well (100 μL medium). The complexes of eGFP-encoded mRNA and lipids (azido-DOTAP, DOTAP, the mixture of azido-DOTAP and DOPE, or the mixture of DOTAP and DOPE) were added to the cells. The mass ratio of lipid : mRNA was fixed at 10 : 1 for the DC transfection studies. The molar ratio of azido-DOTAP (or DOTAP) to DOPE was set at 9 : 1. After 48 h, cells were harvested for flow cytometry analysis.

Synthesis of SIINFEKL mRNA

The mRNA encoding SIINFEKL peptide was generated using the HiScribe T7 polymerase *in vitro* transcription system from NEB (Cat: E2040) following the manufacturer's protocol. The template DNAs used in the transcription process were obtained from a commercial vendor. Briefly, the template design includes the coding sequence of the peptides, a T7 polymerase recognition sequence, a start codon, a stop codon, and various UTR sequences. Following *in vitro* transcription, the mRNA molecules were purified using a Monarch RNA clean up kit from NEB (Cat: T2050) following the manufacturer's protocol.

SIINFEKL antigen presentation by BMDC

Day-7 BMDCs were seeded into 96-well plates at a density of 10k per well (100 μL medium). The complexes of SIINFEKL-encoded mRNA and lipids (azido-DOTAP, DOTAP, DOPE, the mixture of azido-DOTAP and DOPE, the mixture of DOTAP and DOPE, or lipofectamine 2000) were added to the cells (100 ng of SIINFEKL mRNA per well). The mass ratio of lipid : mRNA was fixed at 10 : 1 for the DC transfection studies. The molar ratio of azido-DOTAP (or DOTAP) to DOPE was set at 9 : 1. After 48 h, cells were stained with FITC-conjugated anti-CD11c, APC-conjugated anti-MHCI-SIINFEKL, PE/Cy7-conjugated anti-CD86, and fixable viability dye efluor780. Cells were then washed and resuspended in FACS buffer containing 0.4% PFA for flow cytometry analysis.

Statistical analyses

Statistical analysis was performed using GraphPad Prism v6 and v8. Sample variance was tested using the *F* test. For samples with equal variance, the significance between the

groups was analyzed by a two-tailed Student's *t*-test. For samples with unequal variance, a two-tailed Welch's *t*-test was performed. For multiple comparisons, a one-way analysis of variance (ANOVA) with *post hoc* Fisher's LSD test was used. The results were deemed significant at $0.01 < {}^{*}P \leq 0.05$, highly significant at $0.001 < {}^{**}P \leq 0.01$, and extremely significant at ${}^{***}P \leq 0.001$.

Data availability

Raw data can be accessed upon request and will be published at the Illinois Data Bank upon the acceptance of the manuscript.

Conflicts of interest

The authors declare no competing interests.

Acknowledgements

The authors would like to acknowledge the financial support from NSF DMR 21-43673 CAR (H. W.), NIH R01CA274738 (H. W.), NIH R21CA270872 (H. W.), and start-up package (H. W.) from the Department of Materials Science and Engineering at the University of Illinois at Urbana-Champaign and the Cancer Center at Illinois (CCIL).

References

1 N. Pardi, M. J. Hogan, F. W. Porter and D. Weissman, *Nat. Rev. Drug Discovery*, 2018, **17**, 261–279.
2 L. A. Jackson, *et al.*, *N. Engl. J. Med.*, 2020, **383**, 1920–1931.
3 A. J. Barbier, A. Y. Jiang, P. Zhang, R. Wooster and D. G. Anderson, *Nat. Biotechnol.*, 2022, **40**, 840–854.
4 B. B. Mendes, *et al.*, *Nat. Rev. Methods Primers*, 2022, **2**, 24.
5 E. Samaridou, J. Heyes and P. Lutwyche, *Adv. Drug Delivery Rev.*, 2020, **154**, 37–63.
6 J. A. Kulkarni, S. B. Thomson, S. Chen, B. R. Leavitt, P. R. Cullis and R. van der Meel, *Nat. Nanotechnol.*, 2021, **16**, 630–643.
7 N. Pardi, S. Tuyishime, H. Muramatsu, K. Kariko, B. L. Mui, Y. K. Tam, T. D. Madden, M. J. Hope and D. Weissman, *J. Controlled Release*, 2015, **217**, 345–351.
8 M. J. Evers, J. A. Kulkarni, R. van der Meel, P. R. Cullis, P. Vader and R. M. Schiffelers, *Small Methods*, 2018, **2**, 1700375.
9 L. Schoenmaker, D. Witzigmann, J. A. Kulkarni, R. Verbeke, G. Kersten, W. Jiskoot and D. J. Crommelin, *Int. J. Pharm.*, 2021, **601**, 120586.
10 X. Hou, T. Zaks, R. Langer and Y. Dong, *Nat. Rev. Mater.*, 2021, **6**, 1078–1094.
11 B. Dalby, S. Cates, A. Harris, E. C. Ohki, M. L. Tilkins, P. J. Price and V. C. Ciccarone, *Methods*, 2014, **33**, 95–103.
12 F. Cardarelli, L. Digiacomo, C. Marchini, A. Amici, F. Salomone, G. Fiume, A. Rossetta, E. Gratton, D. Pozzi and G. Caracciolo, *Sci. Rep.*, 2016, **6**, 25879.
13 H. Wang and D. J. Mooney, *Nat. Chem.*, 2020, **12**, 1102–1114.
14 J. M. Baskin, J. A. Prescher, S. T. Laughlin, N. J. Agard, P. V. Chang, I. A. Miller, A. Lo, J. A. Codelli and C. R. Bertozzi, *Proc. Natl. Acad. Sci. U. S. A.*, 2007, **104**, 16793–16797.
15 P. V. Chang, D. H. Dube, E. M. Sletten and C. R. Bertozzi, *J. Am. Chem. Soc.*, 2010, **132**, 9516–9518.
16 S. T. Laughlin, N. J. Agard, J. M. Baskin, I. S. Carrico, P. V. Chang, A. S. Ganguli, M. J. Hangauer, A. Lo, J. A. Prescher and C. R. Bertozzi, *Methods Enzymol.*, 2006, **415**, 230–250.
17 S. T. Laughlin and C. R. Bertozzi, *Nat. Protoc.*, 2007, **2**, 2930.
18 H. Wang, R. Wang, K. Cai, H. He, Y. Liu, J. Yen, Z. Wang, M. Xu, Y. Sun, X. Zhou, Q. Yin, L. Tang, I. T. Dobrucki, L. W. Dobrucki, E. J. Chaney, S. A. Boppart, T. M. Fan, S. Lezmi, X. Chen, L. Yin and J. Cheng, *Nat. Chem. Biol.*, 2017, **13**, 415.
19 R. Xie, L. Dong, Y. Du, Y. Zhu, R. Hua, C. Zhang and X. Chen, *Proc. Natl. Acad. Sci. U. S. A.*, 2016, **113**, 5173–5178.
20 H. Wang, M. C. Sobral, D. Zhang, A. N. Cartwright, A. W. Li, M. O. Dellacherie, C. M. Tringides, S. T. Koshy, K. W. Wucherpfennig and D. J. Mooney, *Nat. Mater.*, 2020, **19**, 1244–1252.
21 J. Han, R. Bhatta, Y. Liu, Y. Bo, A. Elosegui-Artola and H. Wang, *Nat. Commun.*, 2023, **14**, 5049.
22 C. Agatemor, M. J. Buettner, R. Ariss, K. Muthiah, C. T. Saeui and K. J. Yarema, *Nat. Rev. Chem.*, 2019, **3**, 605–620.
23 C. Y. Jao, M. Roth, R. Welti and A. Salic, *Proc. Natl. Acad. Sci. U. S. A.*, 2009, **106**, 15332–15337.
24 A. B. Neef and C. Schultz, *Angew. Chem., Int. Ed.*, 2009, **48**, 1498–1500.
25 C. F. Ancajas, T. J. Ricks and M. D. Best, *Chem. Phys. Lipids*, 2020, **232**, 104971.
26 I. Nilsson, S. Y. Lee, W. S. Sawyer, C. M. B. Rath, G. Lapointe and D. A. Six, *J. Lipid Res.*, 2020, **61**, 870–883.
27 T. Tamura, A. Fujisawa, M. Tsuchiya, Y. Shen, K. Nagao, S. Kawano, Y. Tamura, T. Endo, M. Umeda and I. Hamachi, *Nat. Chem. Biol.*, 2020, **16**, 1361–1367.
28 L. Kuerschner and C. Thiele, *Biochim. Biophys. Acta, Mol. Cell Biol. Lipids*, 2014, **1841**, 1031–1037.
29 A. Laguerre and C. Schultz, *Curr. Opin. Cell Biol.*, 2018, **53**, 97–104.
30 W. Yu, Z. Lin, C. M. Woo and J. M. Baskin, *ACS Chem. Biol.*, 2021, **17**, 3276–3283.
31 T. W. Bumpus, D. Liang and J. M. Baskin, *Methods Enzymol.*, 2020, **641**, 75–94.
32 D. Liang, K. Wu, R. Tei, T. W. Bumpus, J. Ye and J. M. Baskin, *Proc. Natl. Acad. Sci. U. S. A.*, 2019, **116**, 15453–15462.

33 D. C. Chiu and J. M. Baskin, *JACS Au*, 2022, **2**, 2703–2713.
34 J. Yu, H. Zhang, Y. Li, S. Sun, J. Gao, Y. Zhong, D. Sun and G. Zhang, *Biomed. Chromatogr.*, 2017, **31**, e4036.
35 J. Guo, S. Amini, Q. Lei, Y. Ping, J. O. Agola, L. Wang, L. Zhou, J. Cao, S. Franco, A. Noureddine, A. Miserez, W. Zhu and C. J. Brinker, *ACS Nano*, 2022, **16**, 2164–2175.
36 V. T. Ressler, K. A. Mix and R. T. Raines, *ACS Chem. Biol.*, 2019, **14**, 599–602.
37 M. B. Jones, H. Teng, J. K. Rhee, N. Lahar, G. Baskaran and K. J. Yarema, *Biotechnol. Bioeng.*, 2004, **85**, 394–405.
38 D. R. Parle, F. Bulat, S. Fouad, H. Zecchini, K. M. Brindle, A. A. Neves and F. J. Leeper, *Bioconjugate Chem.*, 2022, **33**, 1467–1473.